aptara | GJI | gji_5362 | Dispatch: February 4, 2012 | CE: AFL
Journal | MSP No. | No. of pages: 17 | PE: JM

Geophys. J. Int. (2012) doi: 10.1111/j.1365-246X.2012.05362.x

Distortion decomposition of the magnetotelluric impedance tensors from a one-dimensional anisotropic Earth

Alan G. Jones

Dublin Institute for Advanced Studies, 5 Merrion Square, Dublin 2, Ireland. E-mail: alan@cp.dias.ie

Accepted 2012 January 02. Received 2011 October 7; in original form 2011 May 15

SUMMARY

The Earth is anisotropic at all scales, and models and interpretations of electrical anisotropy from observations are becoming more common. The magnetotelluric (MT) impedance tensor from an arbitrary 1-D anisotropic layered Earth admits an unusual form of six parameters (three complex impedances) with diagonal terms that are equal but of opposite sign. This particular form, somewhat unappreciated and neglected to date, can be exploited to deal with regional MT data that are distorted by galvanic effects of near-surface scatterers. Following prior distortion decomposition approaches, a method is proposed that statistically tests for its validity and solves for the determinable parts of the galvanic distortion and recovers the regional 1-D anisotropic responses. The method is demonstrated on synthetic data and real MT data from two different locations.

Key words: Electrical properties; Electromagnetic theory; Magnetotelluric.

1 INTRODUCTION

Anisotropy—the directional dependence of material properties—is an important manifestation of penetrative tectonic fabrics (e.g. Eaton & Jones 2006). Rock fabrics induced by tectonic processes, particularly, but not exclusively, by lateral plate tectonic translations, provide important clues about the petrogenesis and the deformation history of a region (e.g. Tommasi *et al.* 1999). Unfortunately, our direct knowledge of particularly subcontinental lithospheric fabrics is severely limited by the scarcity and bias of mantle samples, which leaves a significant observational gap in our understanding of dynamics of tectonic processes—in particular, how continents formed and interacted with underlying mantle regions in the past, and how they do so today. This gap can be filled by appropriate geophysical observations of lithospheric anisotropy, and thus geophysical observations of anisotropy, particularly seismic and electrical anisotropy, are providing essential data of lithospheric fabrics and key constraints for geodynamic models of the Earth (e.g. Becker *et al.* 2006).

Continental seismic anisotropy has been studied for well over two decades, with shear wave splitting analyses of core-traversing teleseismic waves (SKS and SKKS arrivals) providing the most comprehensive observational data set (Silver 1996; Savage 1999; Park & Levin 2002). More recently, seismic anisotropy deduced from surface wave studies and receiver functions are also providing important insights (e.g. Gung *et al.* 2003; Endrun *et al.* 2011).

Electromagnetic observations of long-period magnetotelluric (MT) signals provide the best available method to measure electrical anisotropy of the lithospheric and sublithospheric (asthenospheric) mantle. Electrical anisotropy has been interpreted in MT observations, from Mareschal *et al.*'s (1995) key contribution and that of Kurtz *et al.* (1993) to more recent studies (Boerner *et al.* 2000; Simpson 2001; Bahr & Simpson 2002; Leibecker *et al.* 2002; Gatzemeier & Moorkamp 2005; Hamilton *et al.* 2006; Padilha *et al.* 2006). Electrical anisotropy has also been observed in the crust, with the most convincing and compelling example being that of Heise & Pous (2003) in which the anisotropic nature of the lower crust was magnified by the near-surface, fault-generated anisotropy. Miensopust & Jones (2011) discuss the consequences of crustal anisotropic fabrics that align at an angle to regional geoelectrical strike and are not appropriately taken into account. Wannamaker (2005) gives an excellent review of the topic of manifestations of electrical anisotropy and the problem of differentiating between fabric and structural anisotropy.

A caution though was expressed by Jones (2006) that MT practitioners cannot, without care, simply adopt prevailing methods in seismology, especially SKS, and display supposed electrical anisotropy information at a particular period over a large region. The one or more orders of magnitude variation in conductivity that is possible in the presence of either structural or fabric anisotropy, in contrast to a few per cent in velocity, means that penetration depths can vary significantly over large regions, and indeed in the two orthogonal directions at a single site. Maps of geoelectric strike at even the longest periods can be misleading because of crustal effects. Mareschal *et al.* (1995) recognized this problem and plotted their anisotropy information (most conducting azimuths and phase differences between orthogonal directions) at two different periods (42 and 113 s), depending on site location on either side of 81° W. This penetration depth 'problem' (it is only a problem if it

is ignored) was brought into sharp focus more recently by Lahti *et al.* (2005) who demonstrated that crustal effects observed in Fennoscandia can account for observed strike directions deduced from phase differences at even very long (presumed mantle penetrating) periods. Lahti *et al.*'s (2005) observation called into question Bahr & Simpson's (2002) purported mapping of asthenospheric flow beneath Scandinavia, based on Bahr and Simpson's geoelectric strikes observed at 2049 s. More recent studies, such as Hamilton *et al.* (2006); Padilha *et al.* (2006); Jones *et al.* (2009) and Miensopust *et al.* (2011) compensated for varying depth penetration laterally in their studies.

Of course, when the MT data are formally modelled anisotropically, rather than displayed and qualitatively interpreted, these issues do not exist, and 1-D, 2-D and 3-D forward approaches and algorithms have been published (1-D: Sinha 1969; Loewenthal & Landisman 1973; Shoham & Loewenthal 1975; Dekker & Hastie 1980; Li & Pedersen 1992; Yin & Maurer 2001; Pek & Santos 2002, 2-D: Osella & Martinelli 1993; Pek & Verner 1997; Li 2002, 3-D: Martinelli & Osella 1997; Weiss & Newman 2002). Anisotropic 1-D inversion codes have been published (Abramovici & Shoham 1977; Pek & Santos 2006), with the restriction that the axes of anisotropy are horizontal and vertical to avoid non-uniqueness problems (Yin 2003), and that of Pek and Santos, which is based on the Occam approach (Constable *et al.* 1987), is publicly available. A limited anisotropic 2-D inversion code is restrictedly available (Baba *et al.* 2006), extending the isotropic 2-D non-linear conjugate gradient algorithm of Rodi & Mackie (2001), where the limitation is that the anisotropy directions are parallel and perpendicular to regional electrical structural strike. Miensopust & Jones (2011) raise a caution about this assumption in the general case. A generalized 2-D anisotropic inversion does not exist, although J. Pek *et al.* are completing one (Pek *et al.* 2011).

Intriguing correlations between seismic and electrical anisotropy directions have been reported since the seminal work of Ji *et al.* (1996) across the Grenville Front (Canada) demonstrating the remarkably consistent obliquity between the seismic (SKS defined) and electrical (MT defined) horizontal anisotropy directions interpreted in terms of fossil flow processes. Eaton *et al.* (2004) studied the Great Slave Lake shear zone (GSLsz) where no such seismic–electrical obliquity was found; the seismic and electrical directions were parallel. The explanation for this difference between the Grenville Front and GSLsz anisotropy observations comes from the discussion by Tommasi *et al.* (1999) that obliquity between the LPO direction (presumed seismic anisotropy axis) and the foliation direction (presumed electrical anisotropy axis) in olivine will be zero in regions of very low or high shear strain (where the GSLsz falls into the latter category).

A technique for formal joint inversion of seismic (surface wave) and electromagnetic (MT) data for 1-D anisotropy in the crust, lithospheric mantle and sublithospheric (asthenospheric) mantle was presented recently by Roux *et al.* (2011), and there are exciting and interesting problems still to be solved relating seismic and electrical anisotropy together.

MT studies are clearly increasing making insights into Earth processes in terms of anisotropic interpretations. However, galvanic distortion effects, which can plague MT data and are routinely treated in isotropic modelling and inversion in 1-D and 2-D, have not been taken into account in any of the studies to date except that of Hamilton *et al.* (2006) who used a 2-D distortion decomposition in pseudo-depth mode to derive anisotropic information. Hamilton *et al.*'s (2006) approach is only valid though in the case of a layered Earth with a single anisotropic layer within it, as discussed below.

The phase tensor method of Caldwell *et al.* (2004), which avoids the problem of galvanic distortion completely through constructing a tensor based on phases alone, is equally applicable in the case of anisotropic media as it is for isotropic media (Heise *et al.* 2006). However, lost in the phase tensor approach is direct knowledge of bulk conductivity as a direct consequence of discarding half of the information in the MT impedance tensor, namely that half that contains the amplitude information. It is far better to have a technique that retains as much information as possible for accurate and reliable resolution of Earth structure.

Given the availability and use of 3-D inversion codes, one may question the utility of undertaking 1-D anisotropic inversion of data. However, 3-D inversions are currently rather coarse, given the high computational requirements, and also appropriate galvanic distortion identification and removal approaches are, as yet, undeveloped (Jones 2011). Thus approximate methods can have value. Recently, comparative modelling studies by Schmoldt and Jones (Schmoldt 2011; Schmoldt & Jones 2011) demonstrate the utility of anisotropic 1-D modelling of 3-D structures; one can obtain approximate models that contain the dominant features of the 3-D Earth.

Herein I present a technique, based on MT tensor decomposition, for testing whether the regional response can be characterized as that from an arbitrary 1-D anisotropic Earth structure, and for identifying and removing the effects of galvanic distortion from the observed impedance tensors to yield regional MT impedances consistent with the model assumptions. The technique is applied to both synthetic and real data, and its advantages and shortcomings are demonstrated.

2 THEORY

2.1 Forms of the MT impedance tensor

The MT impedance tensor relates the orthogonal horizontal components of the electric and magnetic fields through a 2×2 complex tensor, viz.,

$$\underline{\mathbf{E}} = \underline{\underline{\mathbf{Z}}} \cdot \underline{\mathbf{H}} \tag{1}$$

(dependence on frequency assumed). The impedance tensor assumes three well-known forms depending on the dimensionality of the subsurface.

Q3

2.1.1 *One-dimensional impedance tensor*

In 1-D, that is, a stack of isotropic layers, the impedance tensor becomes

$$\underline{\underline{\mathbf{Z}}}_{1-D} = \begin{bmatrix} 0 & Z_{xy} \\ -Z_{xy} & 0 \end{bmatrix}, \tag{2}$$

where the diagonals are zero and the off-diagonals are equal but of opposite sign (to ensure consistency with the right-hand rule in electromagnetic induction). There are two parameters per frequency, which are the real and imaginary parts of the complex impedance Z_{xy}.

2.1.2 *Two-dimensional impedance tensor*

In 2-D, that is, with resistivity constant along one axis (usually x) in the direction of geoelectric strike of the 2-D structures, the tensor becomes

$$\underline{\underline{\mathbf{Z}}}_{2-\mathrm{D}} = \begin{bmatrix} 0 & Z_{xy} \\ Z_{yx} & 0 \end{bmatrix}, \tag{3}$$

comprizing four parameters (two complex impedances) per frequency. The observed coordinate system is often not aligned to structural strike, so a fifth, frequency-independent parameter, namely the obliquity between the observation reference system and geoelectric strike, θ, needs to be defined, where

$$\begin{aligned} \underline{\underline{\mathbf{Z}}}_{2-\mathrm{D}}(\theta) &= \underline{\underline{\mathbf{R}}} \cdot \underline{\underline{\mathbf{Z}}}_{2-\mathrm{D}}(0) \cdot \mathbf{R}^T \\ &= \begin{bmatrix} \cos(\theta) & \sin(\theta) \\ -\sin(\theta) & \cos(\theta) \end{bmatrix} \begin{bmatrix} 0 & Z_{xy}(0) \\ Z_{yx}(0) & 0 \end{bmatrix} \begin{bmatrix} \cos(\theta) & -\sin(\theta) \\ \sin(\theta) & \cos(\theta) \end{bmatrix} \\ &\begin{bmatrix} \cos(\theta)\sin(\theta)\left[Z_{xy}(0)+Z_{yx}(0)\right] & \cos^2(\theta)Z_{xy}(0) - \sin^2(\theta)Z_{yx}(0) \\ \cos^2(\theta)Z_{yy}(0) - \sin^2(\theta)Z_{xx}(0) & -\cos(\theta)\sin(\theta)\left[Z_{xy}(0)+Z_{yx}(0)\right] \end{bmatrix}. \end{aligned} \tag{4}$$

Note that $Z_{yy}(\theta) = -Z_{xx}(\theta)$, so that

$$\underline{\underline{\mathbf{Z}}}_{2-\mathrm{D}}(\theta) = \begin{bmatrix} Z_{xx}(\theta) & Z_{xy}(\theta) \\ Z_{yx}(\theta) & -Z_{xx}(\theta) \end{bmatrix}. \tag{5}$$

2.1.3 *Three-dimensional impedance tensor*

In 3-D the impedance tensor is full,

$$\underline{\underline{\mathbf{Z}}}_{3-\mathrm{D}}(\theta) = \begin{bmatrix} Z_{xx} & Z_{xy} \\ Z_{yx} & -Z_{yy} \end{bmatrix} \tag{6}$$

and there are eight parameters (four complex impedances) per frequency.

2.1.4 *One-dimensional anisotropic impedance tensor*

Far less known and appreciated, even within the MT community, is a fourth form of the impedance tensor, and that is the one that the tensor assumes over a general 1-D anisotropic Earth in which there are multiple anisotropic layers with differing anisotropy directions. This form is given by

$$\underline{\underline{\mathbf{Z}}}_{1-\mathrm{D}a} = \begin{bmatrix} Z_{xx} & Z_{xy} \\ Z_{yx} & -Z_{yy} \end{bmatrix}, \tag{7}$$

and comprises six parameters (three complex impedances) per frequency, where the diagonal terms are equal but of opposite sign. Vozoff (1972), in his definitive review paper that established the MT method in the early-1970s, presents this form (his eq. 9) as found through computation, and Shoham & Loewenthal (1975) state that it is a consequence of the symmetry of the layer conductivity tensors. This form was shown to be valid in the general case in the theoretical development of Kováčiková & Pek (2002), given in their Appendix A, and also in eqs (30a) and (30d) of Pek & Santos (2002).

The general form of $\underline{\underline{\mathbf{Z}}}_{1-\mathrm{D}a}$ (eq. 7), of six parameters, should not be confused with the rotated form of $\underline{\underline{\mathbf{Z}}}_{2-\mathrm{D}}$ (eq. 3) given by $\underline{\underline{\mathbf{Z}}}_{2-\mathrm{D}}(\theta)$of eq. (5), of five parameters, even though the two appear similar. It is always possible in the 2-D case to find a real-valued rotation angle θ that rotates $\underline{\underline{\mathbf{Z}}}_{2-\mathrm{D}}(\theta)$ such that it can be anti-diagonalized. This is not possible in the general case of layered anisotropic media.

In their book on magnetotellurics, Simpson and Bahr state 'Mathematically, a 1-D anisotropic Earth is equivalent to a 2-D Earth' (Simpson & Bahr 2005, p. 35). This is not true in the general case, only in the limited case where there exists only one anisotropic layer within

the stack of 1-D layers, with all others being isotropic, or in the case where there are multiple anisotropic layers within the stack but they all have the same anisotropy axes. In both of these, then the general form of $\underline{\underline{\mathbf{Z}}}_{1-\mathrm{D}a}$(eq. 7) reduces to the 2-D form $\underline{\underline{\mathbf{Z}}}_{2-\mathrm{D}}$ (eq. 3) when the axes are aligned parallel to one of the anisotropy directions.

In the general 2-D or 3-D anisotropic Earth case there is no specific form of the MT impedance tensor; it adopts the full form expressed by eq. (6). For the restricted case of anisotropy in 2-D with the anisotropy directions all parallel to structural strike, as used by Baba *et al.* (2006), then again when the observational coordinate system is aligned with structural/anisotropy strike, the MT tensor adopts the 2-D form of eq. (3).

2.2 Differentiating between one-dimensional anisotropy and two-dimensional structure

Given that the forms of the 1-D anisotropy and 2-D impedance tensors are similar, how does one differentiate between the two and recognize the existence of 1-D anisotropy over 2-D structure? There are essentially three ways:

(1) The vertical magnetic field transfer function is zero over a 1-D anisotropic Earth, but is non-zero over a 2-D Earth.

(2) The horizontal magnetic field transfer functions are unity over a 1-D anisotropic Earth, but are complex and differ from unity over a 2-D Earth.

(3) There is a constant phase difference over a large region for a 1-D anisotropic Earth, whereas a 2-D Earth has maxima in phase difference at lateral discontinuities in conductivity.

The first and third of these were the bases for Mareschal *et al.*'s (1995) interpretation of the existence of anisotropy in the deep crust and upper mantle of the lithosphere of the eastern Superior craton, Canada. Mareschal *et al.*'s paper was the first convincing case for electrical anisotropy made.

If one only has MT data from a single site, then one must determine if there exists an angle θ that antidiagonalizes the impedance tensor over all frequencies. In that case, then either the Earth is anisotropic 1-D with one layer of anisotropy, or multiple anisotropic layers but with the same anisotropy axes, or is 2-D. If no frequency-independent angle θ can be found, then one can ask whether a model of the Earth comprizing 1-D anisotropic layers is appropriate. These questions have to be posed within a statistical framework, taking galvanic distortion into account.

2.3 Galvanic distortion of the MT impedance tensor

Measurement of the regional horizontal electric fields is notoriously difficult because local, near-surface variations, where 'local' and 'near-surface' are functions of both experimental scale and inductive scale, can distort them through scattering by the effects of charges on conductivity gradients. This distortion is the bane of the MT method, and was first studied in detail by the Russian school under M. Berdichevsky (Berdichevsky & Dmitriev 1976). At sufficiently long periods (low frequencies) where the inductive response of the scatterers can be neglected and the magnetic effects of the charges on the conductivity gradients and boundaries are also negligible, then only the electric field components are affected and the distortion can be described by a real, frequency-independent, 2×2 scattering tensor $\underline{\underline{\mathbf{C}}}$. The treatise of Chave & Smith (1994) mathematically establishes this particularly well and discuss the conditions for applicability of the assumptions.

Larsen (1977) was the first to propose this approach for dealing with effects on Hawaii because of ocean currents, where he was trying to recover the regional 1-D response affected by distortion, viz.,

$$\underline{\underline{\mathbf{Z}}}_{\mathrm{obs}} = \underline{\underline{\mathbf{C}}}\,\underline{\underline{\mathbf{Z}}}_{1-\mathrm{D}}, \tag{8}$$

an equation now in six unknowns at a single period, the four real values of $\underline{\underline{\mathbf{C}}}$ plus the two values of the impedance tensor element Z_{xy}. Over n periods, there are $8n$ knowns (the observed data) and $4 + 2n$ unknowns (the model parameters), as the elements of $\underline{\underline{\mathbf{C}}}$ are frequency-independent.

Richards *et al.* (1982) were the first to describe local distortion of electric fields from a 2-D regional Earth, and thus extended a distortion description to

$$\underline{\underline{\mathbf{Z}}}_{\mathrm{obs}} = \underline{\underline{\mathbf{C}}}\,\underline{\underline{\mathbf{Z}}}_{2-\mathrm{D}}, \tag{9}$$

which, in an arbitrary observation coordinate system, is

$$\underline{\underline{\mathbf{Z}}}(\theta)_{\mathrm{obs}} = \underline{\underline{\mathbf{R}}}(\theta)\underline{\underline{\mathbf{C}}}\,\underline{\underline{\mathbf{Z}}}_{2-\mathrm{D}}\underline{\underline{\mathbf{R}}}^{\mathrm{T}}(\theta), \tag{10}$$

where θ is the direction between 2-D regional strike and the observation axes, $\underline{\underline{\mathbf{R}}}(\theta)$ denotes the Cartesian rotation tensor and superscript T denotes transpose. At a single frequency, this is an equation of nine unknowns and eight knowns, but over n frequencies it is $5 + 4n$ unknowns (as the strike direction θ and the galvanic distortion parameters are all frequency-independent) and $8n$ knowns. In the strike coordinate system, the off-diagonal terms have the correct phase, but are static shifted (Jones 1988), so the main emphasis of many approaches has been to devise methods to determine the regional strike in some optimum manner.

Bahr (1984, 1988) used the rotational properties of eq. (10) and proposed that the angle be sought in which the two elements in each column have the same phase, that is, $\phi_{xx} = \phi_{yx}$ and $\phi_{xy} = \phi_{yy}$. Many others have proposed schemes for determining the strike direction and recovering the 2-D regional impedances, including Zhang *et al.* (1987), Groom & Bailey (1989), Chave & Smith (1994) and Smith (1995).

In the general 3-D case, then

$$\underline{\underline{\mathbf{Z}}}_{\rm obs} = \underline{\underline{\mathbf{C}}}\,\underline{\underline{\mathbf{Z}}}_{\rm 3-D}, \tag{11}$$

which will always be underdetermined as there are for n frequencies $4 + 8n$ unknowns and only $8n$ knowns. Garcia & Jones (2002) proposed that this problem can be addressed when there are pairs of sites for periods where the two sites should be seeing the same regional 3-D structure. Thus, there are $8 + 8n$ unknowns and $16n$ knowns at n frequencies at the two sites.

For the case of 1-D anisotropic Earth, then the distortion is

$$\underline{\underline{\mathbf{Z}}}_{\rm obs} = \underline{\underline{\mathbf{C}}}\,\underline{\underline{\mathbf{Z}}}_{\rm 1-D}a \tag{12}$$

which comprises $4 + 6n$ unknowns for $8n$ knowns at n frequencies. Thus a minimum of two frequencies are required. This paper describes a method to solve for the unknown parameters in eq. (12).

2.4 Distortion decomposition of the MT impedance tensor over a one-dimensional anisotropic Earth

Of the various approaches suggested to determine regional strike and recover the regional 2-D impedances in the case of distortion of a 2-D Earth (eq. (3)), that of Groom and Bailey (Bailey & Groom 1987; Groom & Bailey 1989, 1991; Groom *et al.* 1993) offers the most advantages, particularly the extended multisite, multifrequency implementation of McNeice & Jones (1996, 2001) that is in widespread use. Justifiably, the Groom & Bailey (1989) paper is one of the top most cited in magnetotellurics. Besides posing the problem as one of statistical model-fitting and thereby hypothesis testing as to whether the assumed model is appropriate and of demonstrating the uniqueness of their decomposition, Groom and Bailey proposed a tensor decomposition that separates the scattering tensor $\underline{\underline{\mathbf{C}}}$ into determinable and indeterminable parts; essentially those that are determinable affect phases and amplitudes, whereas those that are indeterminable affect amplitudes only, so cannot be uniquely recovered. The Groom–Bailey decomposition is in terms of a scaling factor and three matrices, given by

$$\begin{aligned}\underline{\underline{\mathbf{C}}} &= g\underline{\underline{\mathbf{T}}}\,\underline{\underline{\mathbf{S}}}\,\underline{\underline{\mathbf{A}}} \\ &= g\begin{bmatrix} 1 & -t \\ t & 1 \end{bmatrix}\begin{bmatrix} 1 & s \\ s & 1 \end{bmatrix}\begin{bmatrix} 1+a & 0 \\ 0 & 1-a \end{bmatrix}\end{aligned} \tag{13}$$

where g is site gain, t is a rotation tensor called twist, s (e in the original paper of Groom & Bailey 1989) is an ellipticity or shearing tensor called shear and a (s in the original paper of Groom & Bailey 1989) is a splitting or anisotropy tensor called anisotropy (herein referred to as distortion anisotropy to differentiate it from model anisotropy). The twist and shear parameters are usually displayed as angles, given by their arctangents.

The two factors g and $\underline{\underline{\mathbf{A}}}$ only affect amplitudes, and a scaled version of $\underline{\underline{\mathbf{Z}}}_{\rm 2-D}$ given by $\underline{\underline{\mathbf{Z}}}'_{\rm 2-D} = g\underline{\underline{\mathbf{A}}}\,\underline{\underline{\mathbf{Z}}}_{\rm 2-D}$ cannot be differentiated from the true $\underline{\underline{\mathbf{Z}}}_{\rm 2-D}$ as the phases are correct and only amplitudes are shifted. This is the classic static shift problem in MT (Jones 1988). Thus, for a 2-D regional Earth then

$$\begin{aligned}\underline{\underline{\mathbf{Z}(\theta)}}_{\rm obs} &= \underline{\underline{\mathbf{R}}}(\theta)\underline{\underline{\mathbf{C}}}\,\underline{\underline{\mathbf{Z}}}_{\rm 2-D}\underline{\underline{\mathrm{R}^{\rm T}}}(\theta) \\ &= \underline{\underline{\mathbf{R}}}(\theta)g\underline{\underline{\mathbf{T}}}\,\underline{\underline{\mathbf{S}}}\,\underline{\underline{\mathbf{A}}}\,\underline{\underline{\mathbf{Z}}}_{\rm 2-D}\underline{\underline{\mathrm{R}^{\rm T}}}(\theta) \\ &= \underline{\underline{\mathbf{R}}}(\theta)\underline{\underline{\mathbf{T}}}\,\underline{\underline{\mathbf{S}}}\,\underline{\underline{\mathbf{A}}}\,\underline{\underline{\mathbf{Z}}}'_{\rm 2-D}\underline{\underline{\mathrm{R}^{\rm T}}}(\theta),\end{aligned} \tag{14}$$

which is an equation of seven unknowns (θ, t and s and the two regional impedances, Z_{xy} and Z_{yx}) and eight knows at one frequency and $3 + 4n$ unknowns and $8n$ knowns at n frequencies. A methodology for applying this approach was given by Groom *et al.* (1993) and working tool for applying it to a regional data set by McNeice & Jones (2001).

For solving the problem of galvanic distortion of electric fields over a 3-D regional Earth (eq. 11), Garcia & Jones (2002) also adopted the same tensor decomposition. However, their approach worked well for synthetic data, but the results indicated that the problem was more intractable and highlighted the difficulties that resulted as a consequence of inherent parameter-resolution instabilities.

In the case of a regional 1-D anisotropic Earth, then the distortion can be described by

$$\begin{aligned}\underline{\underline{\mathbf{Z}}}_{\rm obs} &= \underline{\underline{\mathbf{C}}}\,\underline{\underline{\mathbf{Z}}}_{\rm 1-D}a \\ &= g\underline{\underline{\mathbf{T}}}\,\underline{\underline{\mathbf{S}}}\,\underline{\underline{\mathbf{A}}}\,\underline{\underline{\mathbf{Z}}}_{\rm 1-D}a \\ &= \underline{\underline{\mathbf{T}}}\,\underline{\underline{\mathbf{S}}}\,\underline{\underline{\mathbf{A}}}\,\underline{\underline{\mathbf{Z}}}'_{\rm 1-D}a \\ &= \begin{bmatrix} 1 & -t \\ t & 1 \end{bmatrix}\begin{bmatrix} 1 & s \\ s & 1 \end{bmatrix}\begin{bmatrix} 1+a & 0 \\ 0 & 1-a \end{bmatrix}\underline{\underline{\mathbf{Z}}}'_{\rm 1-D}a,\end{aligned} \tag{15}$$

where $\underline{\underline{\mathbf{Z}}}'_{\rm 1-D}a$ is a scaled version of the true anisotropic 1-D impedance given by $\underline{\underline{\mathbf{Z}}}'_{\rm 1-D}a = g\underline{\underline{\mathbf{Z}}}_{\rm 1-D}a$, as only the site gain can be absorbed into the scaled regional impedance as an indeterminable parameter. Any distortion anisotropy a will result in the mixing of the impedance tensor

elements, viz.,

$$\begin{aligned}\underline{\underline{\mathbf{Z}}}_{\rm obs} &= \underline{\underline{\mathbf{C}}}\,\underline{\underline{\mathbf{Z}}}_{\rm 1-D}a \\ &= \underline{\underline{\mathbf{A}}}\,\underline{\underline{\mathbf{Z}}}_{\rm 1-D}a \\ &= \begin{bmatrix} 1+a & 0 \\ 0 & 1-a \end{bmatrix}\begin{bmatrix} Z_{xx} & Z_{xy} \\ Z_{yx} & -Z_{xx} \end{bmatrix} \qquad \begin{bmatrix} (1+a)Z_{xx} & (1+a)Z_{xy} \\ (1-a)Z_{yx} & -(1-a)Z_{xx} \end{bmatrix}\end{aligned} \tag{16}$$

(for distortion with s and $t = 0$ and $g = 1$) and the diagonal terms are no longer the same magnitude but of opposite sign, as required by eq. (5) and anisotropy can be recognized. Thus, at a single frequency there are nine unknowns (t, s, a and the three complex regional impedances, Z_{xx}, Z_{xy} and Z_{yx}), but only eight knowns. However, at n frequencies there are $\underline{3} + 6n$ unknowns (as t, s and a are all frequency-independent) and $8n$ knowns, thus even for a pair of frequencies there is one degree of freedom and solutions can be sought.

Note that in the case of strong distortion such that the shear value is unity ($s = 1$, i.e. a shear of $\pm 45^\circ$), then

$$\begin{aligned}\underline{\underline{\mathbf{Z}}}_{\rm obs} &= \underline{\underline{\mathbf{C}}}\,\underline{\underline{\mathbf{Z}}}_{\rm 1-D}a \\ &= \underline{\underline{\mathbf{S}}}\,\underline{\underline{\mathbf{Z}}}_{\rm 1-D}a \\ &= \begin{bmatrix} 1 & 1 \\ 1 & 1 \end{bmatrix}\begin{bmatrix} Z_{xx} & Z_{xy} \\ Z_{yx} & -Z_{xx} \end{bmatrix} \\ &= \begin{bmatrix} Z_{yx}+Z_{xx} & Z_{xy}-Z_{xx} \\ Z_{yx}+Z_{xx} & Z_{xy}-Z_{xx} \end{bmatrix} \\ &= \begin{bmatrix} 1 & 1 \\ 1 & 1 \end{bmatrix}\begin{bmatrix} 0 & Z_{xy}-Z_{xx} \\ Z_{yx}+Z_{xx} & 0 \end{bmatrix} \\ &= \underline{\underline{\mathbf{S}}}\,\underline{\underline{\mathbf{Z}}}'_{\rm 2-D}\end{aligned} \tag{17}$$

(for distortion with $a = t = 0$ and $g = 1$). Thus, with $s = 1$ the shear tensor is singular, and the product with the regional impedance tensor is singular so its form is inherently non-unique. This means that in the case of strong shear anisotropy, a distorted impedance tensor from an anisotropic 1-D Earth cannot be differentiated from an equivalent distorted impedance tensor from an isotropic 2-D Earth.

2.5 Implementation of the one-dimensional anisotropic Earth distortion decomposition of the MT impedance tensor

Choice of parametrization is crucial for developing a numerically stable and useful tool for distortion decomposition of MT impedance tensors over a 1-D anisotropic Earth, just as it was for 2-D and 3-D regional Earths. Groom & Bailey (1989) chose a parametrization in terms of sums and differences of the diagonal and off-diagonal elements (their eqs 33). For the 1-D anisotropic Earth, such a parametrization would result in mixing of all three impedances. Following the work of Garcia & Jones (2002) for the 3-D regional Earth case, the parametrization adopted is one of the complex sums and differences of the columns of the MT impedance tensor, namely,

$$\begin{aligned}&\alpha_0 = Z_{xx,\rm obs} - Z_{yx,\rm obs}, \quad \alpha_1 = Z_{xx,\rm obs} + Z_{yx,\rm obs}, \\ &\alpha_2 = Z_{xy,\rm obs} - Z_{yy,\rm obs}, \quad \alpha_3 = Z_{xy,\rm obs} - Z_{yy,\rm obs},\end{aligned} \tag{18}$$

(dependence on frequency assumed). From eq. (15), these parameters are, in terms of their solutions,

$$\begin{aligned}\alpha_0(\omega) &= (1+a)(1-s-t-ts)Z_{xx}(\omega) + (1-a)(-1+s-t-ts)Z_{yx}(\omega) + \varepsilon_0(\omega) \\ \alpha_1(\omega) &= (1+a)(1+s+t-ts)Z_{xx}(\omega) + (1-a)(+1+s-t+ts)Z_{yx}(\omega) + \varepsilon_1(\omega) \\ \alpha_2(\omega) &= (1+a)(1-s-t-ts)Z_{xy}(\omega) + (1-a)(+1-s+t+ts)Z_{xx}(\omega) + \varepsilon_2(\omega) \\ \alpha_3(\omega) &= (1+a)(1+s+t-ts)Z_{xy}(\omega) + (1-a)(-1-s+t-ts)Z_{xx}(\omega) + \varepsilon_3(\omega)\end{aligned} \tag{19}$$

where ε_i are the (complex) errors of misfit of the model parameters (t, s, a and the three complex regional impedances, Z_{xx}, Z_{xy} and Z_{yx}) to the observations. Equations (16) are a system of $8n$ non-linear equations (one for the real and imaginary parts for each α) with $3 + 6n$ unknowns at n frequencies ω.

To ensure stability and that the solutions are not dominated by the high frequency data, given the natural decrease in impedance with decreasing frequency (increasing period), the alphas at each frequency are normalized by the largest real or imaginary alpha at that frequency.

A solution is sought that minimizes the sum of squares of the misfits over n frequencies, namely

$$f = \sum_{i=1}^{n}\sum_{j=0}^{3}\varepsilon_j^2 \tag{20}$$

using a bounded, quasi-Newton algorithm. The hard bounds that can be applied are to the shear parameter s; it must lie in the range ± 1. Loose bounds are applied to the other parameters.

The χ^2 misfit of the determined distortion and anisotropy parameters are in the usual manner from

$$\chi^2 = \sum \frac{|Z_{ij,\mathrm{obs}} - Z_{ij,\mathrm{mod}}|}{\sigma_{ij}^2} \tag{21}$$

for $i,j = x,y$. From this the standard root mean square (rms) is derived by dividing χ^2 by $8n$ (number of data) and taking the square root and the reduced rms (rrms) from dividing χ^2 by $[8n - (3 + 6n)]$; number of degrees of freedom in the model fitting, given by $8n$ minus $(3 + 6n)$ model parameters] and taking the square root.

Errors on the parameters are derived robustly using a bootstrap, resampling approach (Efron 1979) with typically 100 realizations created randomly from the observed values and their given errors.

3 SYNTHETIC EXAMPLE

The synthetic example chosen to demonstrate the algorithm is one discussed in Jones (2006) to describe the MT responses observed over the GSLsz in northwestern Canada. The model comprises four layers, with an isotropic upper crust, an anisotropic lower crust and anisotropic lithospheric mantle, with different anisotropy directions and an isotropic asthenosphere (Table 1). The MT responses of this model were derived over six decades of period, from 0.01 to 10 000 s with 10 estimates per decade, using the forward code of Pek & Santos (2002) based on the algorithm of Kováčiková & Pek (2002) and are shown in Fig. 1.

To these 61 model data are added Gaussian scatter and noise (with noise added to the error estimates) at the 3.5 per cent in impedance level (approx. 7 per cent in apparent resistivity and 2° in phase) and distortion given by a of the form

$$\underline{\underline{\mathbf{C}}} = \begin{bmatrix} 1.26 & 0.532 \\ 0.558 & 0.760 \end{bmatrix}, \tag{22}$$

which is a gain g of 1.0, a distortion anisotropy (a) of 0.20, a twist (t) of –0.0875 (twist angle of –5°) and a shear (s) of 0.577 (shear angle of +30°). These synthetic data are shown in Fig. 2. Note that the distortion destroys the form of the MT impedance tensor from that in eq. (7);

Table 1. Model values of synthetic 1-D anisotropic GSLsz.

Layer	Thickness (km)	Rho-x (Ωm)	Rho-y (Ωm)	Rho-z (Ωm)	θ of Rho-x
Upper crust	10	10 000	10 000	10 000	N/A
Lower crust	30	300	10 000	300	30
Lithospheric mantle	160	30	1000	30	60
Asthenosphere	N/A	30	30	30	N/A

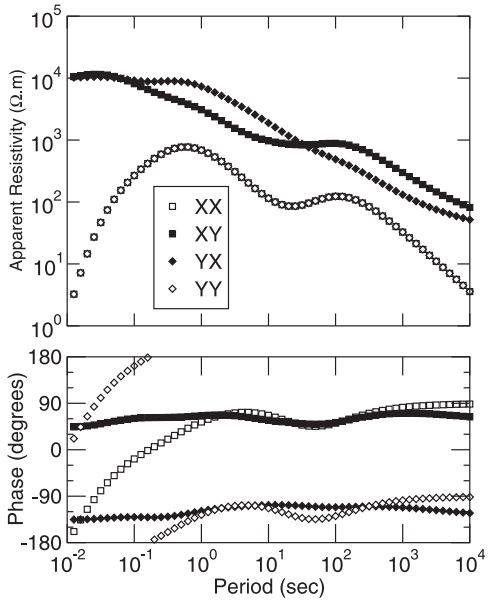

Figure 1. MT forward response of the synthetic 1-D anisotropic GSLsz model given in Table 1.

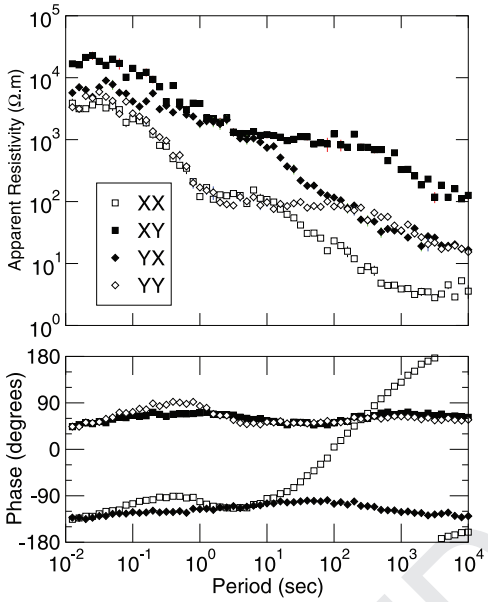

Figure 2. Synthetic data created from the model data in Fig. 1 after adding scatter, noise and distortion.

the diagonal impedances are not the same amplitudes with a phase difference of 180°. One could not confidently conclude that these data result from a 1-D anisotropic Earth.

Applying Occam's Razor, one must determine the simplest possible model that fits these data to within their statistical limits. Clearly, there is either 3-D structure or distortion (or both) present, so neither the undistorted 1-D (eq. 2), 1-D with anisotropy (eq. (7)) nor 2-D (eq. (5)) forms are appropriate. Next must be to determine if a model of 3-D galvanic distortion of 2-D regional Earth is acceptable. To ascertain this, the 3-D/2-D multifrequency galvanic tensor distortion removal method of McNeice & Jones (2001) is first applied to these data, which yields the strike, shear and twist shown in Fig. 3, together with the plotted rms misfit. The galvanic distortion parameters derived are:

$$\text{strike} = +77.33^\circ(77.44^\circ - 77.22^\circ)$$

$$t = +2.40^\circ(2.36^\circ - 2.44^\circ)$$

$$s = +23.25^\circ(23.22^\circ - 23.28^\circ).$$

The shear and twist estimates are somewhat close to their correct values of $+30^\circ$ and -5°, respectively, but the *s*trike direction is not consistent with either the lower crust direction ($+30^\circ$) or the upper mantle direction ($+60^\circ$). The model, of 3-D galvanic distortion of data from a 2-D regional Earth, does not though fit the data statistically. The average and median rms are 1.52 and 1.40 respectively, which may be thought acceptable, but only 22 of the 61 estimates (36 per cent) are below 1.0, rather than 68 per cent (one sigma) and only 40 of the 61 estimates (66 per cent) are below 2.0, rather than 95 per cent (two sigma). In addition, when judging whether a model fits the data, one should not be solely guided by rms misfit however, but consider higher order measures of model fit to the data. Particularly indicative of the poor fit is the 'colour' of the misfit; all data at periods <3 s have misfits greater than 2.0. The Durbin–Watson statistic (Durbin & Watson, 1950) for serial correlations yields a value of 0.37 for the residual rms values, well outside the 5 per cent significance level for uncorrelated residuals of 1.97–2.03.

Applying the galvanic distortion scheme described above for 3-D distortion of data from a 1-D anisotropic regional Earth, to these data analysis yields estimates of the distortion parameters as follows:

$$t = -4.49^\circ[-4.53^\circ - (-4.46^\circ)]$$

$$s = +28.78^\circ(28.7^\circ - 28.9^\circ)$$

$$a = 0.19(0.187 - 0.192)$$

and the recovered regional impedances as shown in Fig. 4. The 488 model data (8 data at 61 periods) fit the observations with an acceptable average and median rms of 1.21 and 1.02 respectively, with 50 per cent (30 of 61) below 1.0, and 83 per cent (51 of 61) below 2.0 and without any significant serial correlations in the residuals (Durbin–Watson statistic of 1.37). The algorithm is able to recover successfully the regional impedances and also the distortion parameters.

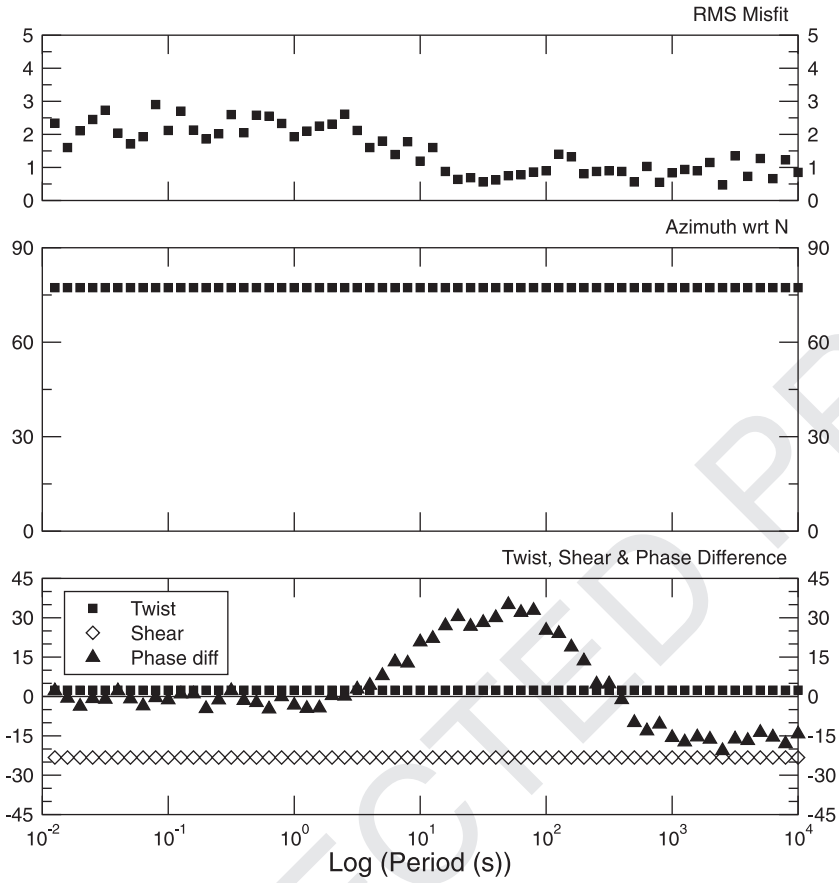

Figure 3. Recovered distortion parameters (strike, shear, twist), phase differences and rms misfit for the data from Fig. 2 applying a model of 3-D galvanic distortion of a 2-D regional Earth.

4 APPLICATION TO REAL DATA

4.1 Site DIE

Site DIE lies in central Germany, and was examined in detail in the recent publication of Roux *et al.* (2011). The data from site DIE comprise MT responses at 18 periods from 10 to 3000 s, and are representative of the anisotropic structure of the crust and upper mantle beneath central Germany (Leibecker *et al.* 2002; Gatzemeier & Moorkamp 2005). The situation in central Germany is the same as central Superior Province, where the results of Mareschal *et al.* (1995) demonstrated the regional extent of the lithospheric anisotropy, that is, the third type of evidence for differentiating between 2-D structure and anisotropic 1-D. The data are shown in Fig. 5, and the necessary requirement of the form of the impedance tensor for $Z_{xx} = -Z_{yy}$ is clearly not obeyed, raising the question about the appropriateness of interpreting the data as resulting from a 1-D anisotropic Earth.

For model fitting, an error floor of 3.5 per cent in impedance (equal to 7 per cent in apparent resistivity and 2° in phase) was used. Errors smaller than this were increased to 3.5 per cent, whereas errors that were larger were unaltered.

A model of 3-D galvanic distortion of a 2-D regional Earth best fits the data with the parameters shown in Fig. 6. The strike and galvanic distortion parameters twist and shear are

$$\text{strike} = \pm 43.67^\circ[(-42.90^\circ) - (-44.44^\circ)]$$

$$t = -4.95^\circ[(-4.90^\circ) - (-4.99^\circ)]$$

$$s = -3.34^\circ[(-3.14^\circ) - (-3.54^\circ)].$$

These are low values of distortion. However, the averaged rms error is relatively high, at 1.35, with only 22 per cent below 1.0 and 68 per cent below 2.0 and the Durbin–Watson statistic of 0.76 is indicative of correlated residuals. This 3-D/2-D model does not statistically fit the data to within the errors.

Allowing unconstrained 1-D anisotropic models fit over pairs of data at neighbouring periods yields parameters shown in Fig. 7(a) with an overall rms of 0.51 (Table 2). Statistically, these models fit the data well as the overall rms is acceptable and there are no strong individual rms values above 2.0, but clearly the distortion parameters twist, shear and anisotropy are not frequency-independent, so the models are not an acceptable description of 3-D/1-D*a* distortion.

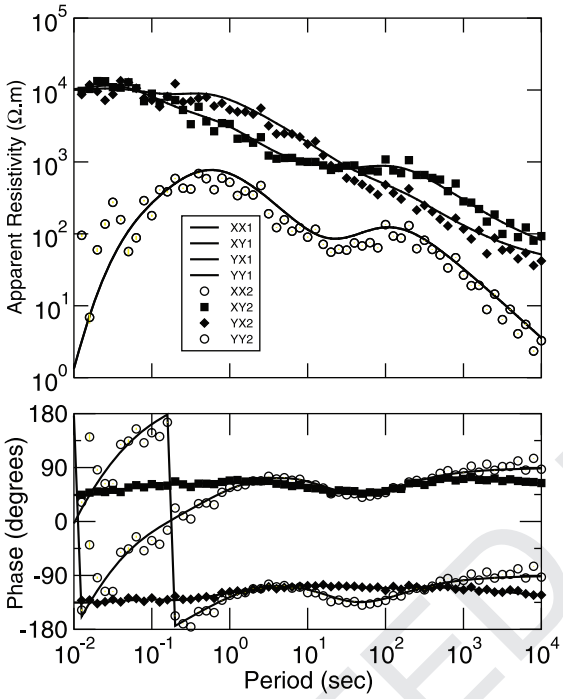

Figure 4. Recovered regional impedances (points) compared to the true values (solid lines) for the data from Fig. 2 applying a model of distortion of a 1-D anisotropic regional Earth.

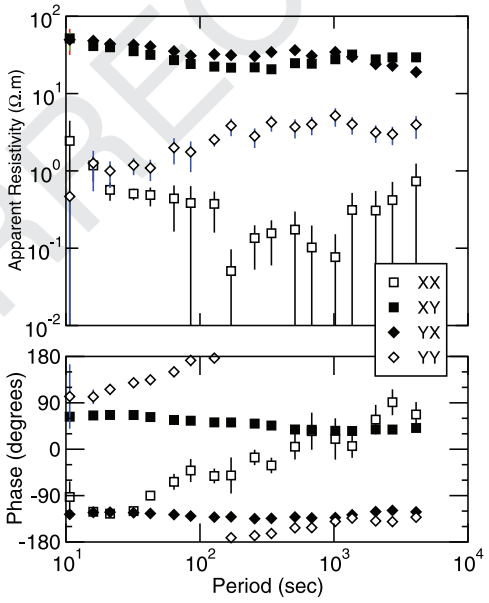

Figure 5. MT data from site DIE in central Germany.

The parameters of the best-fitting model with frequency-independent distortion parameters are given in Table 2. The overall rms is acceptable at 0.73, although there are strong rms values at some periods (Fig. 7b). However, the distortion anisotropy value of –0.4 is a problem as that would result in significant splitting of the off-diagonal apparent resistivities. Given that at short periods the ρ_{xy} and ρ_{yx} resistivities are close to one another, this implies that distortion anisotropy is low to negligible and solutions must be sought with $a = 0.0$.

The best-fitting model with only twist and shear free (but frequency-independent) and distortion anisotropy fixed to 0.0 yields a large overall rms misfit of 1.66, but more than half of the misfit comes from the data at the 3rd, 4th and 5th periods (Fig. 7c). Removing these points and fitting the data at the remaining 15 periods yields an acceptable model with an rms of 0.99 (Table 2), although there is bias in that the short period data are poorly fit. Fitting the data in two bands on either side of 300 s yields the parameters of the best-fitting models listed in Table 2. Note that small variations in the distortion parameters can result in large misfit errors.

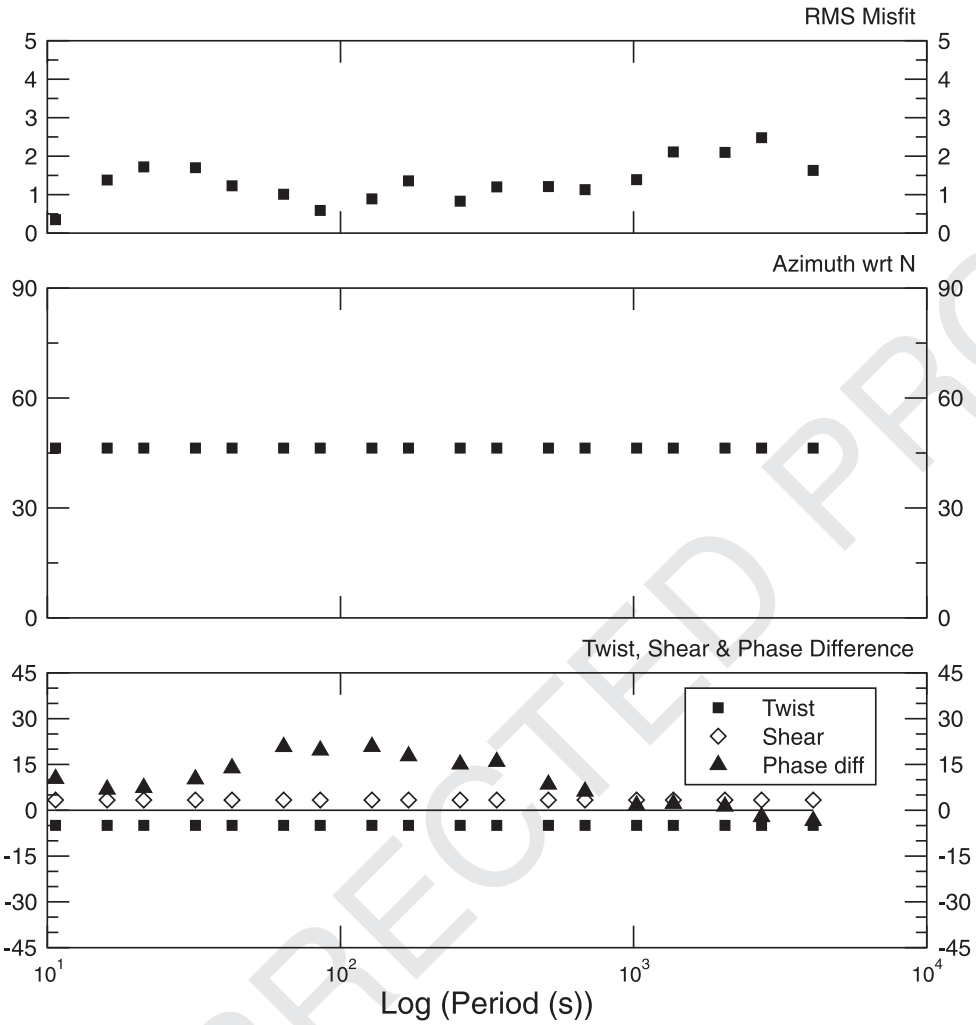

Figure 6. Recovered distortion parameters parameters (strike, shear, twist), phase differences and rms misfit for the data from DIE (Fig. 5) applying a model of 3-D galvanic distortion of a 2-D regional Earth.

Averaging the distortion parameters of the two period bands yields a distortion model adopted, with twist = –8.0°, shear = –5.3° and distortion anisotropy = 0.0, which fits acceptably (rms = 1.01). These values give the regional MT estimates shown in Fig. 8 (symbols), compared with the original distorted estimates (solid lines). Thus, a valid model of distortion can be found that fits the observations, and the recovered regional impedances can be validly interpreted in terms of resulting from an anisotropic 1-D Earth. These data are now suitable for 1-D anisotropic modelling and inversion.

4.2 Site sno156

Site *sno156* lies on top of the GSLsz. The MT data have been modelled and interpreted by Wu *et al.* (2005) and Eaton *et al.* (2004) and formed part of the analysis of Jones (2006) for electromagnetic field penetration problems in orthogonal directions. The data are shown in Fig. 9, and, although Z_{xx} and Z_{yy} share a similar shape for some of the period range, particularly between 0.1 and 10 s, they are clearly not equal in magnitude at all periods. Again, for model fitting an error floor of 3.5 per cent in impedance was set.

A model of 3-D galvanic distortion of a 2-D regional Earth best fits the data with the parameters shown in Fig. 10. The strike and galvanic distortion parameters twist and shear are

$$\text{strike} = \pm 44.99^\circ[(-44.93^\circ) - (-45.04^\circ)]$$

$$t = -2.33^\circ[(-2.30^\circ) - (-2.36^\circ)]$$

$$s = -6.20^\circ[(-6.15^\circ) - (-6.25^\circ)].$$

Galvanic distortion is very low, but the 3-D/2-D model does not fit the data. The average and median rms are 2.36 and 2.08 respectively, with none below rms = 1.0 and only 37 per cent below rms = 2.0. In addition, the very low Durbin–Watson statistic of 0.48 attests to the high serial correlation of the residuals.

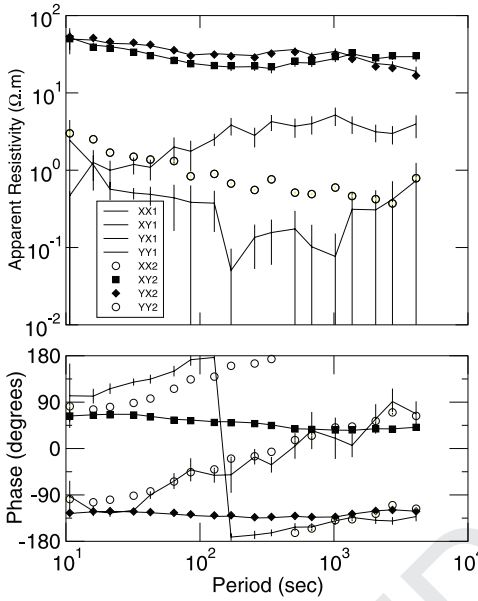

Figure 7. Fit of anisotropic 1-D distortion models to data from site DIE data (Fig. 5). (a): Unconstrained model fitting frequency pairs (shown are the rms values and twist, shear and distortion anisotropy); (b): rms values of model fitting all frequencies; (c): rms values of model fitting all frequencies with distortion anisotropy fixed to 0.0; (d): rms values of model fitting all frequencies but the 3rd, 4th and 5th and with distortion anisotropy fixed to 0.0.

Table 2. Distortion parameters fitting site ***DIE*** for various assumptions and data combinations.

Model	Twist (°)	Shear (°)	Anisotropy	rms
Unconstrained	Varying	Varying	Varying	0.19
All periods	−3.6	−0.3	−0.4	0.72
All periods, $a = 0.0$	−5.6	−3.6	0.0 (fixed)	1.66
All periods except 3rd, 4th and 5th, $a = 0.0$	−6.6	−8.4	0.0 (fixed)	0.99
Periods < 300 s	−8.2	−4.8	0.0 (fixed)	0.59
Periods > 300 s	−7.8	−5.8	0.0 (fixed)	0.43
Adopted distortion model for all periods	−8.0 (fixed)	−5.3 (fixed)	0.0 (fixed)	1.01

An unconstrained 3-D/1-D*a* model fitting over data from pairs of periods yields an rms of 0.23 (Table 3), indicative that it may be possible to find an acceptable model. Fitting a model over all periods however yields a large overall rms misfit of 1.40 (Table 3). This may be thought to be acceptable, except that only 12 of the data at 46 periods have an individual rms below 1, instead of 32 (68 per cent) as required statistically and 28 of them lie between 1.0 and 2.0.

Again though, the high frequency asymptotes of the off-diagonal apparent resistivities, R_{xy} and R_{yx}, indicate that distortion anisotropy is small to negligible, requiring models to be sought with $a = 0.0$. A frequency-independent model with $a = 0.0$ has a much higher overall rms misfit of 5.18 that is certainly not acceptable.

Inspecting the data, there is equivalence in the ρ_{xx} and ρ_{yy} curves in the period band 0.1–10 s. The distortion model for the data in this band, with $a = 0.0$ fixed, fits acceptably with an rms of 1.02 and low distortion; twist = 2.1° and shear = 17.5°. Broadening the band out to higher frequencies (0.005–10 s) yields a model with low distortion and an acceptable misfit (Table 3). The regional curves recovered from the distortion decomposition are plotted in Fig. 11 (curves to 10 s period). These can be validly modelled for anisotropic structure to depths of approx. 40–50 km, that is, the base of the crust.

At longer periods, >20 s, a different model of distortion is found, with an acceptable rms but very high distortion; twist = –14.6° and shear = –44.7°. The distortion here is essentially crustal heterogeneity that has only a galvanic expression at long periods. This strong distortion means that one cannot conclude that the regional MT responses are indicative of a 1-D anisotropic Earth, but could come from a 2-D isotropic Earth. Indeed, an acceptable 3-D/2-D model of distortion can be found to fit these data at these periods that is statistically an equally valid model with an rms = 1.05 and twist = –7.6° and shear = –33.3°.

Applying these distortions independently below (short period) and above (long period) 10 s, plus applying a gain factor *g* of 1/21 to the long period impedance magnitudes, yields the regional MT responses shown in Fig. 11. These curves cannot be modelled together as is, but are indicative of regional conductivity variation. Thus, one can conclude that one can determine models that fit the data, but that the models have limited depth validity.

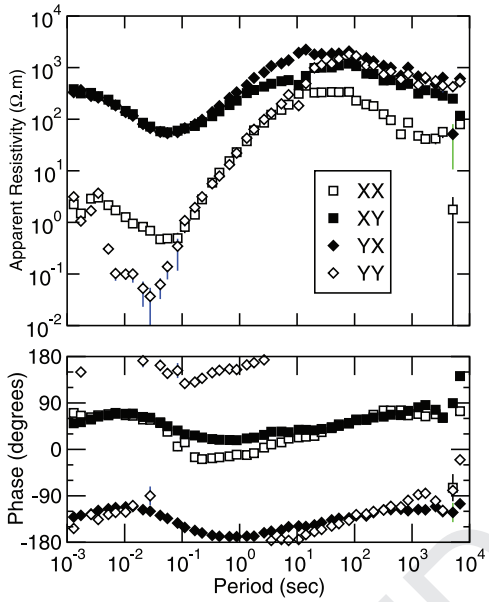

Figure 8. Original data for site DIE (solid lines) compared with recovered data after distortion decomposition (symbols).

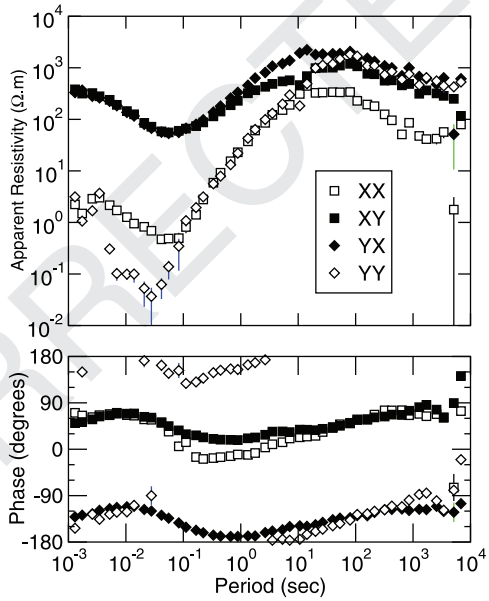

Figure 9. MT data from site sno156 in northern Canada on the Great Slave Lake shear zone.

5 CONCLUSIONS

Distortion of MT data can make valid modelling and interpretation difficult to impossible, and, if ignored, can lead to erroneous conclusions. Techniques for identifying and partially removing the effects of galvanic distortion on the regional horizontal electric field were proposed for regional 1-D structure in the mid-1970s (Larsen 1977), regional 2-D structures in the 1980s (Richards *et al.* 1982; Bahr 1984, 1988; Zhang *et al.* 1987; Bailey & Groom 1987; Groom & Bailey 1989; 1991) and regional 3-D structures in the late-1990s (Garcia & Jones 1999, 2002, Utada & Munekane 2000). With tools such as the multisite, multifrequency distortion decomposition of McNeice and Jones (McNeice & Jones 1996, 2001), MT data are now routinely analysed for distortion effects and the recovered regional impedances modelled.

This paper describes an approach for identifying and removing the effects of distortion where the regional conductivity structure can be validly described by a stack of 1-D anisotropic layers. The approach follows that of Groom & Bailey (1989), but with the parametrization of Garcia & Jones (2002). Synthetic data, constructed from a model response with noise, scatter and distortion added, were analysed with the new tool and the correct distortion factors and regional impedance tensor elements recovered.

MT data from two sites, one in central Germany and the other in northern Canada, were analysed to demonstrate the utility of the approach. In the former case, the data successfully fit a model of distortion over the whole period range, whereas in the latter case the data must be divided into two sets—one for the crust and one for the upper mantle.

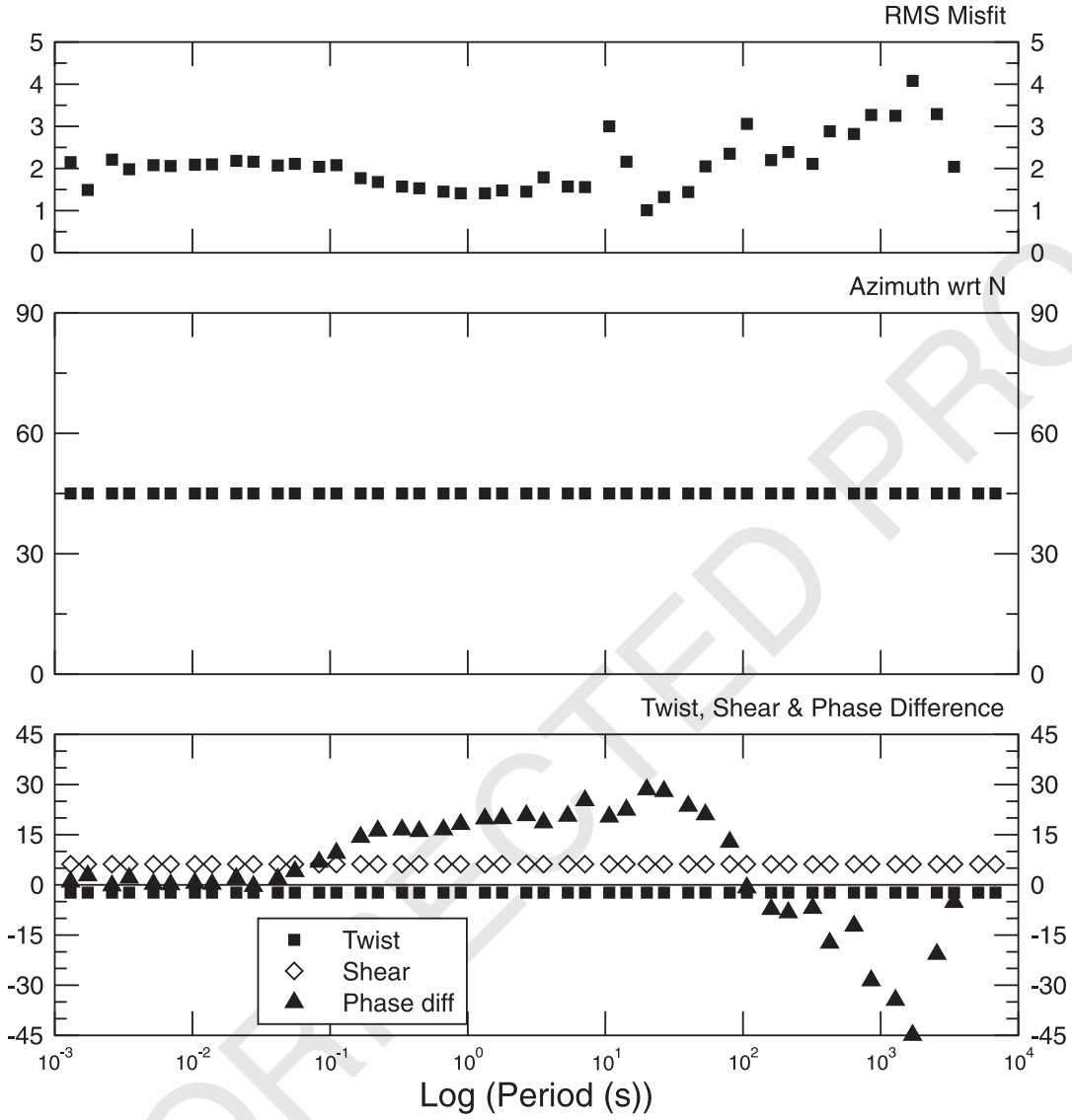

Figure 10. Recovered distortion parameters parameters (strike, shear, twist), phase differences and rms misfit for the data from sno156 (Fig. 9) applying a model of 3-D galvanic distortion of a 2-D regional Earth.

Table 3. Distortion parameters fitting site sno156 for various assumptions and data combinations.

Model	Twist (°)	Shear (°)	Anisotropy	rms
Unconstrained	Varying	Varying	Varying	0.23
All periods	−17.1	−41.9	−0.44	1.40
All periods, $a = 0.0$	−6.2	−43.7	0.0 (fixed)	5.18
Periods 0.1–10 s	28.5	41.3	−0.52	0.75
Periods 0.1–10 s, $a = 0.0$	2.6	17.5	0.0 (fixed)	1.02
Periods 0.005–10 s, $a = 0.0$	2.1	15.0	0.0 (fixed)	0.93
Periods > 20 s, $a = 0.0$	−14.6	−44.7	0.0 (fixed)	1.16
3-D/2-D distortion periods >20 s Strike = –12.3°	−7.6	−33.3	N/A	1.05

ACKNOWLEDGMENTS

This work was undertaken under the auspices of Science Foundation Ireland grant 'Anisotropy of the Continental Lithosphere: Evidence of past tectonics or of active deformation?' (SFI 07/RFP/GEOF759) and was accomplished while the author was at the University of Montpellier 2 as a guest of Professor Andrea Tommasi continuing on a collaboration initiated by an Ireland-France Ulysses travel grant in 2010 to Jones and Tommasi. The author wishes to acknowledge the financial support of SFI, IRCSET and the University of Montpellier 2—Region Languedoc–Roussillon.

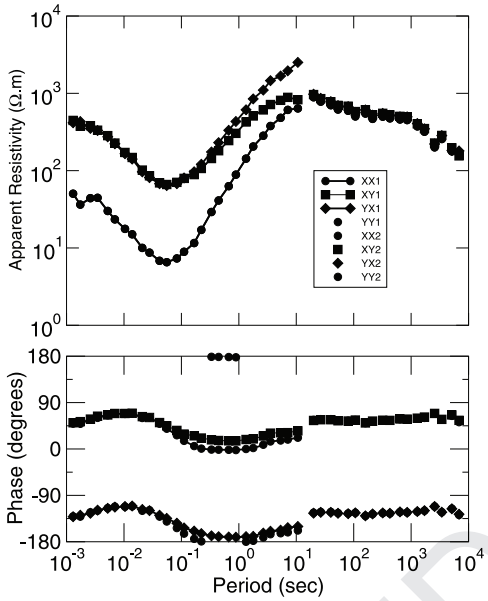

Figure 11. Recovered regional responses for site sno156 (original data in Fig. 9). The decomposition was in two bands below and above 10 s.

Dr. Josef Pek is thanked for providing the forward code for the calculation of responses from a 1-D anisotropic Earth and for many interesting discussions on the topic.

The handling editor, Mark Everett, and two anonymous reviewers are thanked for their suggested improvements to the original version of this manuscript.

REFERENCES

Abramovici, F. & Shoham, Y., 1977. Inversion of anisotropic magnetotelluric data, *Geophys. J. R. astr. Soc.*, ***50***, 55–74.

Baba, K., Chave, A.D., Evans, R.L., Hirth, G. & Mackie, R.L., 2006. Mantle dynamics beneath the east pacific rise at 17 degrees S: insights from the Mantle electromagnetic and tomography (MELT) experiment, *J. geophys. Res-Solid Earth*, **111**, B02101, doi:10.1029/2004jb003598.

Bahr, K., 1984. Elimination of local 3D distortion of the magnetotelluric tensor impedance allowing for two different phases, in *Seventh Workshop on Electromagnetic Induction in the Earth and Moon*, Ile-Ife, Nigeria.

Bahr, K., 1988. Interpretation of the magnetotelluric impedance tensor—regional induction and local telluric distortion, *J. Geophys.*, **62**, 119–127.

Bahr, K. & Simpson, F., 2002. Electrical anisotropy below slow- and fast-moving plates: paleoflow in the upper mantle? *Science*, **295**, 1270–1272.

Bailey, R.C. & Groom, R.W., 1987. Decomposition of the magnetotelluric impedance tensor which is useful in the presence of channeling. in *57th Annual International Society of Exploration Geophysicists Meeting and Exposition*, pp. 154–156, Tulsa, OK.

Becker, T.W., Chevrot, S., Schulte-Pelkum, V. & Blackman, D.K., 2006. Statistical properties of seismic anisotropy predicted by upper mantle geodynamic models, *J. geophys. Res.-Solid Earth*, **111,** B08309, doi:10.1029/2005JB004095.

Berdichevsky, M.N. & Dmitriev, I.V., 1976. Distortion of magnetic and electric fields by near-surface lateral inhomogeneities, *Acta Geod. Geophys. Montan. Acad. Sci. Hung.*, **11**, 447–483.

Boerner, D.E., Kurtz, R.D. & Craven, J.A., 2000. A summary of electromagnetic studies on the Abitibi-Grenville transect, *Can. J. Earth Sci.*, **37**, 427–437.

Caldwell, T.G., Bibby, H.M. & Brown, C., 2004. The magnetotelluric phase tensor, *Geophys. J. Int.*, **158**, 457–469.

Chave, A.D. & Smith, J.T., 1994. On electric and magnetic galvanic distortion tensor decompositions, *J. geophys. Res.-Solid Earth*, **99**, 4669–4682.

Constable, S.C., Parker, R.L. & Constable, C.G., 1987. Occam's inversion: a practical algorithm for generating smooth models from electromagnetic sounding data, *Geophysics*, **52**, 289–300.

Dekker, D.L. & Hastie, L.M., 1980. Magneto-telluric impedances of an anisotropic layered Earth model, *Geophys. J. R. astr. Soc.*, **61**, 11–20.

Durbin, J. & Watson, G.S., 1950. Testing for serial correlation in least squares regression .1, *Biometrika*, **37**, 409–428.

Eaton, D.W. & Jones, A.G., 2006. Tectonic fabric of the subcontinental lithosphere: evidence from seismic, magnetotelluric and mechanical anisotropy—preface, *Phys. Earth planet. Inter.*, **158**, 85–91.

Eaton, D.W., Jones, A.G. & Ferguson, I.J., 2004. Lithospheric anisotropy structure inferred from collocated teleseismic and magnetotelluric observations: Great Slave Lake shear zone, northern Canada, *Geophys. Res. Lett.*, **31**, L19614, doi:10.1029/2004GL020939.

Efron, B., 1979. Bootstrap methods: another look at the jackknife, *Ann. Stat.*, **7**, 1–12.

Endrun, B., Lebedev, S., Meier, T., Tirel, C. & Friederich, W., 2011. Complex layered deformation within the Aegean crust and mantle revealed by seismic anisotropy, *Nat. Geosci.*, **4,** 203–207.

Garcia, X. & Jones, A.G., 1999. Extended decomposition of MT data. in *Second International Symposium on Three-Dimensional Electromagnetics*, Salt Lake City, Utah.

Garcia, X. & Jones, A.G., 2002. Extended decomposition of MT data. in *Three-Dimensional Electromagnetics*, pp. 235–250, eds Zhdanov, M.S. & Wannamaker, P.E., Elsevier.

Gatzemeier, A. & Moorkamp, M., 2005. 3D modelling of electrical anisotropy from electromagnetic array data: hypothesis testing for different upper mantle conduction mechanisms, *Phys. Earth planet. Inter.*, **149**, 225–242.

Groom, R.W. & Bailey, R.C., 1989. Decomposition of magnetotelluric impedance tensors in the presence of local three dimensional galvanic distortion, *J. geophys. Res.*, **94**, 1913–1925.

Groom, R.W. & Bailey, R.C., 1991. Analytical investigations of the effects of near surface three dimensional galvanic scatterers on MT tensor decomposition, *Geophysics*, **56**, 496–518.

Groom, R.W., Kurtz, R.D., Jones, A.G. & Boerner, D.E., 1993. A quantitative methodology for determining the dimensionality of conductive structure from magnetotelluric data, *Geophys. J. Int.*, **115**, 1095–1118.

Gung, Y.C., Panning, M. & Romanowicz, B., 2003. Global anisotropy and the thickness of continents, *Nature*, **422**, 707–711.

Hamilton, M.P. *et al*., 2006. Electrical anisotropy of South African lithosphere compared with seismic anisotropy from shear-wave splitting analyses, *Phys. Earth planet. Inter.*, **158**, 226–239.

Heise, W., Caldwell, T.G., Bibby, H.M. & Brown, C., 2006. Anisotropy and phase splits in magnetotellurics, *Phys. Earth planet. Inter.*, **158**, 107–121.

Heise, W. & Pous, J., 2003. Anomalous phases exceeding 90 degrees in magnetotellurics: anisotropic model studies and a field example, *Geophys. J. Int.*, **155**, 308–318.

Ji, S.C., Rondenay, S., Mareschal, M. & Senechal, G., 1996. Obliquity between seismic and electrical anisotropies as a potential indicator of movement sense for ductile shear zones in the upper mantle, *Geology*, **24**, 1033–1036.

Jones, A.G., 1988. Static shift of magnetotelluric data and its removal in a sedimentary basin environment, *Geophysics*, **53**, 967–978.

Jones, A.G., 2006. Electromagnetic interrogation of the anisotropic Earth: looking into the Earth with polarized spectacles, *Phys. Earth planet. Inter.*, **158,** 281–291.

Jones, A.G., 2011. Three-dimensional galvanic distortion of three-dimensional regional conductivity structures: comments on "three-dimensional joint inversion for magnetotelluric resistivity and static shift distributions in complex media" by Y. Sasaki and M.A. Meju (2006)", *J. geophys. Res.-Solid Earth*, **116**, B12104, doi:10.1029/2011JB008665.

Jones, A.G. *et al*., 2009. Area selection for diamonds using magnetotellurics: examples from southern Africa, *Lithos*, **112**, 83–92, doi:10.1016/j.lithos.2009.06.011.

Kovacikova, S. & Pek, J., 2002. Generalized Riccati equations for 1-D magnetotelluric impedances over anisotropic conductors Part I: plane wave field model, *Earth planets Space*, **54**, 473–482.

Kurtz, R.D., Craven, J.A., Niblett, E.R. & Stevens, R.A., 1993. The conductivity of the crust and mantle beneath the Kapuskasing uplift—electrical anisotropy in the upper mantle, *Geophys. J. Int.*, **113**, 483–498.

Lahti, I., Korja, T., Kaikkonen, P., Vaittinen, K. & Grp, B.W., 2005. Decomposition analysis of the BEAR magnetotelluric data: implications for the upper mantle conductivity in the Fennoscandian Shield, *Geophys. J. Int.*, **163**, 900–914.

Larsen, J.C., 1977. Removal of local surface conductivity effects from low frequency mantle response curves, *Acta Geod. Geophys. Acad. Sci. Hung.*, **12**, 183–186.

Leibecker, J., Gatzemeier, A., Honig, M., Kuras, O. & Soyer, W., 2002. Evidence of electrical anisotropic structures in the lower crust and the upper mantle beneath the rhenish shield, *Earth planet. Sci. Lett.*, **202**, 289–302.

Li, X.B. & Pedersen, L.B., 1992. Controlled-source tensor magnetotelluric responses of a layered Earth with azimuthal anisotropy, *Geophys. J. Int.*, **111**, 91–103.

Li, Y.G., 2002. A finite-element algorithm for electromagnetic induction in two-dimensional anisotropic conductivity structures, *Geophys. J. Int.*, **148**, 389–401.

Loewenthal, D. & Landisman, M., 1973. Theory for magnetotelluric observations on the surface of a layered anisotropic half space, *Geophys. J. R. astr. Soc.*, **35**, 195–214.

Mareschal, M., Kellett, R.L., Kurtz, R.D., Ludden, J.N., Ji, S. & Bailey, R.C., 1995. Archean cratonic roots, mantle shear zones and deep electrical anisotropy, *Nature*, **375**, 134–137.

Martinelli, P. & Osella, A., 1997. MT forward modeling of 3-D anisotropic electrical conductivity structures using the Rayleigh-Fourier method, *J. Geomag. Geoelectr*, **49**, 1499–1518.

McNeice, G. & Jones, A.G., 1996. Multisite, multifrequency tensor decomposition of magnetotelluric data, in *66th Society of Exploration Geophysicists Annual General Meeting*, Denver, Colorado.

Q9

McNeice, G.W. & Jones, A.G., 2001. Multisite, multifrequency tensor decomposition of magnetotelluric data, *Geophysics*, **66**, 158–173.

Miensopust, M.P. & Jones, A.G., 2011. Artefacts of isotropic inversion applied to magnetotelluric data from an anisotropic Earth, *Geophys. J. Int.*, **187**, 677–689, doi:10.1111/j.1365-246X.2011.05157.x.

Miensopust, M.P., Jones, A.G., Muller, M.R., Garcia, X. & Evans, R.L., 2011. Lithospheric structures and precambrian terrane boundaries in northeastern Botswana revealed through magnetotelluric profiling as part of the southern African magnetotelluric experiment, *J. geophys. Res.-Solid Earth*, **116**, B02401, doi:10.1029/2010jb007740.

Osella, A.M. & Martinelli, P., 1993. Magnetotelluric response of anisotropic 2-D structures, *Geophys. J. Int.*, **115**, 819–828.

Padilha, A.L., Vitorello, I., Padua, M.B. & Bologna, M.S., 2006. Lithospheric and sublithospheric anisotropy beneath central-southeastern Brazil constrained by long period magnetotelluric data, *Phys. Earth planet. Inter.*, **158**, 190–209.

Park, J. & Levin, V., 2002. Geophyics–seismic anisotropy: tracing plate dynamics in the mantle, *Science*, **296**, 485–489.

Pek, J. & Santos, F.A.M., 2002. Magnetotelluric impedances and parametric sensitivities for 1-D anisotropic layered media, *Comput. Geosci.*, **28**, 939–950.

Pek, J. & Santos, F.A.M., 2006. Magnetotelluric inversion for anisotropic conductivities in layered media, *Phys. Earth planet. Inter.*, **158**, 139–158.

Pek, J., Santos, F.A.M. & Li, Y., 2011. Magnetotelluric inversion for 2-D anisotropic conductivity. in *EGU*, Vienna, Austria.

Q10

Pek, J. & Verner, T., 1997. Finite-difference modelling of magnetotelluric fields in two-dimensional anisotropic media, *Geophys. J. Int.*, **128**, 505–521.

Richards, M.L., Schmucker, U. & Steveling, E., 1982. Entzerrung der Impedanzkurven von magnetotellurischen Messungen in der Schwabischen Alb. in *Elektromagnetische Tiefenforschung*, pp. 27–40.

Q11

Rodi, W. & Mackie, R.L., 2001. Nonlinear conjugate gradients algorithm for 2-D magnetotelluric inversion, *Geophysics*, **66**, 174–187.

Roux, E., Moorkamp, M., Jones, A.G., Bischoff, M., Endrun, B., Lebedev, S. & Meier, T., 2011. Joint inversion of long-period magnetotelluric data and surface-wave dispersion curves for anisotropic structure: application to data from Central Germany, *Geophys. Res. Lett.*, **38**, L05304, doi:10.1029/2010GL046358.

Savage, M.K., 1999. Seismic anisotropy and mantle deformation: what have we learned from shear wave splitting?, *Rev. Geophys.*, **37**, 65–106.

Schmoldt, J.-P., 2011. *Multidimensional isotropic and anisotropic investigation of The Tajo Basin subsurface: a novel anisotropic inversion approach for subsurface cases with oblique geoelectric strike directions*, *Ph.D. thesis*, National University of Ireland, Galway, Galway.

Q12

Schmoldt, J.-P. & Jones, A.G., 2011. A novel anisotropic inversion approach for magnetotelluric data from subsurfaces with oblique geoelectric strike directions, *Geophys. J. Int.*, in preparation.

Q13

Shoham, Y. & Loewenthal, D., 1975. Matrix polynomial representation of anisotropic magnetotelluric impedance tensor, *Phys. Earth planet. Inter.*, **11**, 128–138.

Silver, P.G., 1996. Seismic anisotropy beneath the continents: probing the depths of geology, *Annu. Rev. Earth planet. Sci.*, **24**, 385–432.

Simpson, F., 2001. Resistance to mantle flow inferred from the electromagnetic strike of the Australian upper mantle, *Nature*, **412**, 632–635.

Simpson, F. & Bahr, K., 2005. *Practical Magnetotellurics*, Cambridge University Press, Cambridge, UK.

Q14

Sinha, A.K., 1969. Magnetotelluric effect in an inhomogeneous and anisotropic Earth, *Geoexploration*, **7**, 9–28.

Smith, J.T., 1995. Understanding telluric distortion matrices, *Geophys. J. Int.*, **122**, 219–226.

Tommasi, A., Tikoff, B. & Vauchez, A., 1999. Upper mantle tectonics: three-dimensional deformation, olivine crystallographic fabrics and seismic properties, *Earth planet. Sci. Lett.*, **168**, 173–186.

Utada, H. & Munekane, H., 2000. On galvanic distortion of regional three-dimensional magnetotelluric impedances, *Geophys. J. Int.*, **140**, 385–398.

Vozoff, K., 1972. The magnetotelluric method in the exploration of sedimentary basins, *Geophysics*, **37**, 98–141.

Wannamaker, P.E., 2005. Anisotropy versus heterogeneity in continental solid earth electromagnetic studies: fundamental response characteristics and implications for physicochemical state, *Surv. Geophys.*, **26**, 733–765.

Weiss, C.J. & Newman, G.A., 2002. Electromagnetic induction in a fully 3-D anisotropic earth, *Geophysics*, **67**, 1104–1114.

Wu, X.H., Ferguson, I.J. & Jones, A.G., 2005. Geoelectric structure of the Proterozoic Wopmay Orogen and adjacent terranes, Northwest Territories, Canada, *Can. J. Earth Sci.*, **42**, 955–981.

Yin, C. & Maurer, H.M., 2001. Electromagnetic induction in a layered earth with arbitrary anisotropy, *Geophysics*, **66**, 1405–1416.

Yin, C.C., 2003. Inherent nonuniqueness in magnetotelluric inversion for 1D anisotropic models, *Geophysics*, **68**, 138–146.

Zhang, P., Roberts, R.G. & Pedersen, L.B., 1987. Magnetotelluric strike rules, *Geophysics*, **52**, 267–278.

Queries

Journal: GJI
Paper: gji_5362

Dear Author

During the copy-editing of your paper, the following queries arose. Please respond to these by marking up your proofs with the necessary changes/additions. Please write your answers on the query sheet if there is insufficient space on the page proofs. Please write clearly and follow the conventions shown on the corrections sheet. If returning the proof by fax do not write too close to the paper's edge. Please remember that illegible mark-ups may delay publication.

Query Reference	Query	Remarks
Q1	Author: please check and confirm that you are happy with the section (shown on the right-hand side of the title page) to which this paper has been assigned: a list of all the sections can be found in the Author Guidelines (http://www.wiley.com/bw/submit.asp?ref=0956-540X&site=1).	
Q2	Author: As per journal style only keywords from the keyword list are allowed. No other keywords are allowed, so we have deleted the keywords 'anisotropy, distortion'. Please confirm.	
Q3	Wiley-Blackwell: As per journal style 1-D should be spelled out in the headings. But in doing so, it exceeds the limit of 45 characters required for the short title provided by the author. Please check.	
Q4	Author: Please supply the editors' name and page range for reference Bahr (1984), or indicate if it is a one-page reference.	
Q5	Author: Please supply the editors' name for reference Bailey & Groom (1987).	
Q6	Author: Please check the inserted volume number for reference Eaton et al. (2004).	
Q7	Author: Please supply the editors' name and page range for reference Garcia & Jones (1999), or indicate if it is a one-page reference.	
Q8	Author: Please provide publisher's location for reference Garcia & Jones (2002).	
Q9	Author: Please supply the editors' name, publisher's name and page range for reference McNeice & Jones (1996), or indicate if it is a one-page reference.	
Q10	Author: Please supply the editors' name, publisher's name and page range for reference Pek et al.(2011), or indicate if it is a one-page reference.	
Q11	Author: Please supply English version of the reference Richards et al.(1982) given in some other language.	

Q12	Author: Please provide page range for reference Schmoldt (2011), or indicate if it is a one-page reference.	
Q13	Author: Please update reference Schmoldt & Jones (2011) with volume number and doi code or page range (or both), or indicate if it is a one-page reference.	
Q14	Author: Please supply the page range (or both) for reference Simpson & Bahr (2005), or indicate if it is a one-page reference.	

Key words

Authors are requested to choose key words from the list below to describe their work. The key words will be printed underneath the summary and are useful for readers and researchers. Key words should be separated by a semi-colon and listed in the order that they appear in this list. An article should contain no more than six key words.

GEOPHYSICAL METHODS
Time series analysis
Image processing
Neural networks, fuzzy logic
Numerical solutions
Fourier analysis
Wavelet transform
Instability analysis
Inverse theory
Numerical approximations and analysis
Persistence, memory, correlations, clustering
Probabilistic forecasting
Spatial analysis
Downhole methods
Tomography
Interferometry
Thermobarometry
Fractals and multifractals
Non-linear differential equations
Probability distributions
Self-organization

GEODESY and GRAVITY
Satellite geodesy
Satellite gravity
Reference systems
Sea level change
Space geodetic surveys
Seismic cycle
Transient deformation
Gravity anomalies and Earth structure
Geopotential theory
Time variable gravity
Earth rotation variations
Global change from geodesy
Lunar and planetary geodesy and gravity
Radar interferometry
Plate motions
Tides and planetary waves
Acoustic-gravity waves

GEOMAGNETISM and ELECTROMAGNETISM
Electrical anisotropy
Electrical properties
Electromagnetic theory
Magnetotelluric
Non-linear electromagnetics
Archaeomagnetism
Biogenic magnetic minerals
Dynamo: theories and simulations
Environmental magnetism
Geomagnetic excursions
Geomagnetic induction
Ground penetrating radar
Magnetic anomalies: modelling and interpretation
Magnetic and electrical properties
Magnetic fabrics and anisotropy
Magnetic field
Magnetic mineralogy and petrology
Magnetostratigraphy
Palaeointensity
Palaeomagnetic secular variation
Palaeomagnetism applied to tectonics
Palaeomagnetism applied to geologic processes
Rapid time variations
Remagnetization
Reversals: process, time scale, magnetostratigraphy
Rock and mineral magnetism
Satellite magnetics
Marine magnetics and palaeomagnetics
Marine electromagnetics

GENERAL SUBJECTS
Geomorphology
Geomechanics
Glaciology
Hydrogeophysics
Ionosphere/atmosphere interactions
Ionosphere/magnetosphere interactions
Gas and hydrate systems
Ocean drilling
Instrumental noise
Hydrology
Ultra-high pressure metamorphism
Ultra-high temperature metamorphism
Tsunamis
Thermochronology
Heat flow
Hydrothermal systems
Mantle processes
Core, outer core and inner core

COMPOSITION and PHYSICAL PROPERTIES
Microstructures
Permeability and porosity
Plasticity, diffusion, and creep
Composition of the core
Composition of the continental crust
Composition of the oceanic crust
Composition of the mantle
Composition of the planets
Creep and deformation
Defects
Elasticity and anelasticity
Equations of state
High-pressure behaviour
Fracture and flow
Friction
Fault zone rheology
Phase transitions

SEISMOLOGY
Controlled source seismology
Earthquake dynamics
Earthquake ground motions
Earthquake source observations
Broad-band seismometers
Seismic monitoring and test-ban treaty verification
Palaeoseismology
Earthquake interaction, forecasting, and prediction
Seismicity and tectonics
Body waves
Surface waves and free oscillations
Interface waves
Guided waves
Coda waves
Seismic anisotropy
Seismic attenuation
Site effects
Seismic tomography
Volcano seismology
Computational seismology
Theoretical seismology
Statistical seismology
Wave scattering and diffraction
Wave propagation
Acoustic properties
Early warning
Rheology and friction of fault zones

TECTONOPHYSICS
Planetary tectonics
Mid-ocean ridge processes
Transform faults
Subduction zone processes
Intra-plate processes
Volcanic arc processes
Back-arc basin processes
Cratons
Continental margins: convergent
Continental margins: divergent
Continental margins: transform
Continental neotectonics
Continental tectonics: compressional
Continental tectonics: extensional
Continental tectonics: strike-slip and transform
Sedimentary basin processes
Oceanic hotspots and intraplate volcanism
Oceanic plateaus and microcontinents
Oceanic transform and fracture zone processes
Submarine landslides
Submarine tectonics and volcanism
Tectonics and landscape evolution
Tectonics and climatic interactions
Dynamics and mechanics of faulting
Dynamics of lithosphere and mantle
Dynamics: convection currents, and mantle plumes
Dynamics: gravity and tectonics
Dynamics: seismotectonics
Heat generation and transport

Impact phenomena
Hotspots
Large igneous provinces
Lithospheric flexure
Obduction tectonics
Neotectonics
Diapir and diapirism
Folds and folding
Fractures and faults
Kinematics of crustal and mantle deformation
High strain deformation zones
Crustal structure
Mechanics, theory, and modelling
Rheology: crust and lithosphere
Rheology: mantle

PLANETS
Planetary interiors
Planetary volcanism

VOLCANOLOGY
Physics of magma and magma bodies
Magma chamber processes
Magma genesis and partial melting
Pluton emplacement
Effusive volcanism
Mud volcanism
Subaqueous volcanism
Explosive volcanism
Volcaniclastic deposits
Volcano/climate interactions
Atmospheric effects (volcano)
Volcanic gases
Lava rheology and morphology
Magma migration and fragmentation
Eruption mechanisms and flow emplacement
Physics and chemistry of magma bodies
Calderas
Experimental volcanism
Tephrochronology
Remote sensing of volcanoes
Volcano monitoring
Volcanic hazards and risks

GEOGRAPHIC LOCATION
Africa
Antarctica
Arctic region
Asia
Atlantic Ocean
Australia
Europe
Indian Ocean
New Zealand
North America
Pacific Ocean
South America

MARKED PROOF

Please correct and return this set

Please use the proof correction marks shown below for all alterations and corrections. If you wish to return your proof by fax you should ensure that all amendments are written clearly in dark ink and are made well within the page margins.

Instruction to printer	*Textual mark*	*Marginal mark*
Leave unchanged	• • • under matter to remain	✓
Insert in text the matter indicated in the margin		New matter followed by or
Delete	/ through single character, rule or underline or ⊢⊣ through all characters to be deleted	 or
Substitute character or substitute part of one or more word(s)	/ through letter or ⊢⊣ through characters	new character / or new characters /
Change to italics	— under matter to be changed	
Change to capitals	≡ under matter to be changed	≡
Change to small capitals	= under matter to be changed	=
Change to bold type	~ under matter to be changed	~
Change to bold italic	≈ under matter to be changed	
Change to lower case	Encircle matter to be changed	
Change italic to upright type	(As above)	
Change bold to non-bold type	(As above)	
Insert ‘superior’ character	/ through character or where required	 or under character e.g. or
Insert ‘inferior’ character	(As above)	 over character e.g.
Insert full stop	(As above)	⊙
Insert comma	(As above)	,
Insert single quotation marks	(As above)	 or and/or or
Insert double quotation marks	(As above)	 or and/or or
Insert hyphen	(As above)	⊢
Start new paragraph		
No new paragraph		
Transpose		
Close up	linking  characters	
Insert or substitute space between characters or words	/ through character or where required	
Reduce space between characters or words	 between characters or words affected